JOURNAL OF MATERIALS SCIENCE 33 (1998) 259–263

Characterization of a solid solution of Cu in Al–Cu–SiC_p metal matrix composites processed by spray atomization and co-deposition

J. A. JUAREZ-ISLAS*, B. CAMPILLO**, R. PEREZ**
** Instituto de Investigaciones en Materiales, ** Facultad de Química, UNAM, Circuito Exterior, Cd. Universitaria, México, 04510, D.F., México*

S. SU, E. J. LAVERNIA
Department of Chemical Engineering and Materials Science, University of California, Irvine, CA 92717-2575, USA

The effect of silicon carbide particulate (SiC_p) reinforcement on the formation of a solid solution of copper (Cu) in Al–Cu alloys during spray atomization and co-deposition is investigated. The extent of Cu solid solubility in sample compositions of Al–1.3, 5.9 and 18.3 wt% Cu and Al–1.5, 5.9 and 19.4 wt% Cu + 6 vol% SiC_p was characterized using X-ray diffraction scanning electron microscopy, (SEM) microanalysis and high resolution electron microscope techniques. The copper content retained in the α-Al solid solution in Al-alloys both with and without SiC_p additions was determined by initially deriving the lattice parameter (*a*) values of the samples by X-ray diffraction and the copper content in the solid solution was determined using a plot of *a* versus copper content previously, reported in the literature. Results of SEM microanalyses performed on the above alloys in regions of α-Al solid solution showed a good agreement on the amount of Cu retained in solid solution with values determined by X-ray diffraction especially for alloys containing small amounts of Cu. High resolution electron microscopy images of the matrix and the matrix/SiC_p interface were employed in order to determine values of the interplanar spacing (*d*) for the α-Al solid solution and to correlate these values using the plot of lattice parameter as a function of copper content retained in solid solution. The results were in good agreement with those determined by the scanning electron microscopy microanalyses.

1. Introduction

Extended solid solubility (ESS) is an important effect encountered with rapid solidification processing techniques [1], in which the solid solubility of a solute element in a matrix alloy can dramatically improve the mechanical behaviour and other properties of the alloy, due to modifications of the sample microstructure. ESS is generally produced by rapid solidification techniques, and it is strongly related to the alloy chemistry [2], thermodynamic properties of the solute element and the matrix alloy [2–4], and kinetic parameters [5–8]. Based on the extensive literature that exists on this subject, it is believed that an extensive solid solubility range can result from a large amount of undercooling or a high cooling rate during solidification [1, 2–5].

Particulate reinforced metal matrix composites (MMC) have received a considerable amount of attention in recent years, due to their combination of a high strength, high Young's modulus, high toughness and low density. In addition, a detailed account of the solid solubility ranges are available in the literature [1, 9, 10]. In the present study, the formation of a supersaturated solid solution during spray atomization and co-deposition of Al–Cu and Al–Cu/SiC_p MMC is investigated. An understanding of the formation of supersaturated solid solubility during spray atomization and co-deposition processing is complicated due to extreme differences in solidification environments, encountered after impact with the deposition surface [11]. The situation is further complicated as a result of the solidification effect produced by the co-injection of a ceramic particulate (such as SiC_p as in the present study) during spray atomization and co-deposition processing [11, 12]. The main objective of the present study is to provide an insight into the effect of the co-deposition of SiC_p on the Cu solid solubility range in α-Al to produce Al–Cu binary alloys. Microstructural effects produced by the SiC_p and the change in alloy chemistry composition with added SiC_p is also investigated.

2. Experimental procedure

The experimental procedure for processing the Al–Cu alloys both with and without added SiC_p used as a

reinforcement via spray atomization and co-deposition techniques has been previously reported [12]. The solidified microstructures were revealed by using normal procedures. The lattice parameters of the Cu–α-Al solid solution were determined using a Siemens D-500 diffractometer with CuK_α radiation at a scanning rate of 2° min^{-1} over the range in diffraction angles of 2–120°.

The Cu concentrations in the cellular α-Al solid solution were determined for each experiment from the mean of at least 10 scanning electron microscope (SEM) microanalysis measurements obtained using a spot size of 64 nm in a Jeol 6400 SEM microscope operated at 15 kV with pure aluminium and pure copper samples used as standards. For the high resolution electron microscope observations, the specimens were electrothinned using a solution of 5% perchloric acid in ethanol at −10 °C, 25 V and 0.12 A, and the observations were performed using a Jeol 4000 high resolution electron microscope.

3. Results and discussion

The chemical analyses of the Al-alloys both with and without SiC_p additions after the spray atomization and co-deposition experiments are listed in Table I. The Cu content in the alloys was fixed on the basis of the Al–Cu phase diagram, so as to produce an Al alloy with a composition in the α-region, another with a composition close to the maximum concentration of Cu in Al at equilibrium, and one sample with a hypo-eutectic composition.

Figs 1(a–b) and 2(a–b) show the microstructures of the Al–Cu alloys both without and with SiC_p, respectively, in the as-spray/co-deposited condition. The microstructure observed in the Al–Cu alloys produced without any SiC_p showed a cellular α-Al solid solution with an intercellular eutectic of the Al_2Cu type. It can be observed that as the Cu content increases (from 1.3 to 18.3 wt %), the amount of the eutectic phase also increases. For the Al–Cu alloys produced with added SiC_p, the observed microstructure was of the cellular type (for the Al–1.14 wt % Cu) without the presence of any eutectic. The SiC_p were observed to exist at the cell boundaries. In the Al–5.9 wt % Cu sample, a cellular type microstructure was observed along with a eutectic. Once again the SiC_p were observed to exist at the cell boundaries. The Al–19.4 wt % Cu sample contained a cellular microstructure plus eutectic and in this case the SiC_p were related with the eutectic.

TABLE I Alloy composition in wt %

Sample 253	Al–1.34 Cu
Sample 254	Al–5.94 Cu
Sample 255	Al–18.29 Cu
Sample 256	Al–1.47 Cu + 6 vol % SiC_p
Sample 257	Al–5.95 Cu + 6 vol % SiC_p
Sample 258	Al–19.43 Cu + 6 vol % SiC_p

The variation of the lattice parameter of the cubic α-Al phase with the extent of solid solution formation with the copper has been obtained by analysis of X-ray diffraction patterns to obtain interplanar, (d) spacings and h, k, l values and hence the lattice parameter, a, was calculated. These values of the lattice parameter are listed in Table II for the Al–Cu alloys both with and without SiC_p together with derived copper contents in solid solution obtained from a plot of the variation of lattice parameters of the f.c.c. α-Al solid solution as a function of copper concentration (see Fig. 3) reported by Fujinaga *et al.* [13]. Note that Fig. 3 is in at %, so in order to convert from wt % to at %, it can be the equation [(wt % cu/atomic wt Cu)]/[(wt % Al/atomic wt Al) + (wt % Cu/atomic wt % Cu)].

Table III lists the copper content in the solid solution determined by SEM microanalyses on the Al–1.34, 5.94 and 18.29 wt % Cu alloys. The low Cu contents retained in solid solution (it has been reported that is possible to retain up to 34 wt % Cu in solid solution by using cooling rates of about 10^6 K s^{-1} [14]) are due to extreme differences in the solidification environment. After impact of these spray/deposited alloys with the deposition surface, it was possible to retain up to 7.32 wt % Cu in solid solution.

The same table shows the effect of the SiC_p on the extent of the Cu solid solution, for the Al–1.47 wt % Cu + SiC_p, it was possible to retain up to 1.28 wt % Cu in solid solution while for the other two alloys (5.95 and 19.43 wt % Cu + SiC_p) the amount of Cu retained in solid solution (3.4 and 6.7 wt % Cu, respectively), is

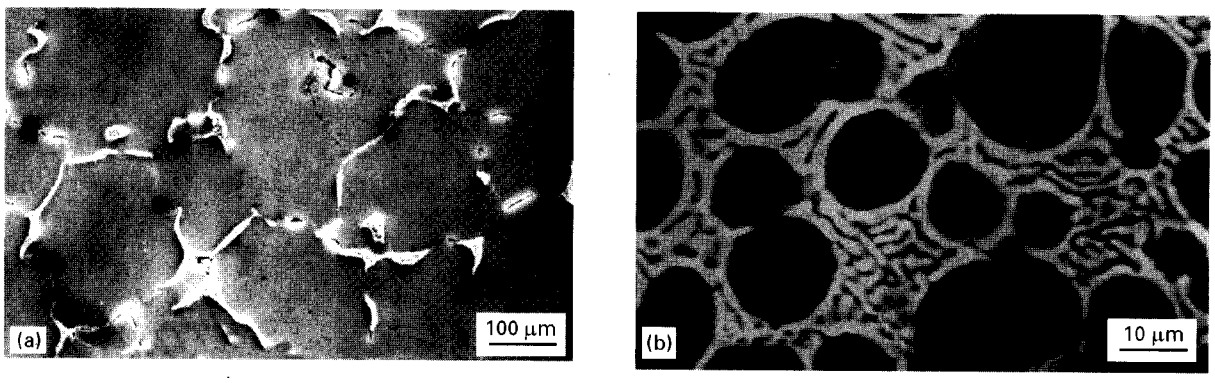

Figure 1 Microstructure of the pure Al–Cu alloy, (a) α-Al solid solution, (b) α-Al matrix and intercellular eutectic.

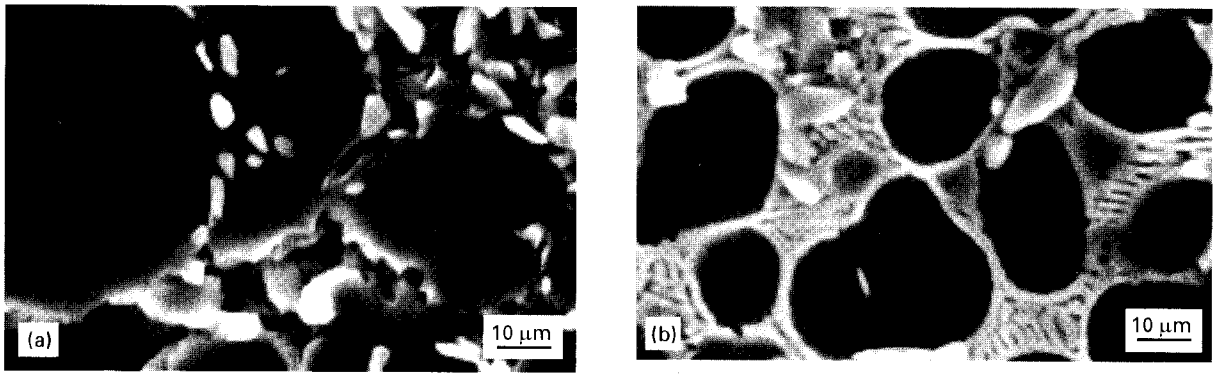

Figure 2 Microstructure of Al–Cu alloy containing SiC_p, (a) α-Al solid solution + SiC_p at interphases, (b) α-Al matrix + intercellular eutectic with SiC_p.

TABLE II Compositional dependence of the lattice parameter

Experiment	Alloy (wt %)	Lattice parameter (nm)	Cu content in solid solution (wt %)
253	Al–1.34	0.40484 ± 0.00002	1.07 ± 0.09
254	Al–5.94	0.40430 ± 0.00002	3.37 ± 0.19
255	Al–18.29	0.40358 ± 0.00003	6.15 ± 0.10
256	Al–1.47 + SiC_p	0.40474 ± 0.00002	1.30 ± 0.09
257	Al–5.95 + SiC_p	0.40433 ± 0.00004	3.32 ± 0.19
258	Al–19.43 + SiC_p	0.40360 ± 0.00004	5.69 ± 0.19

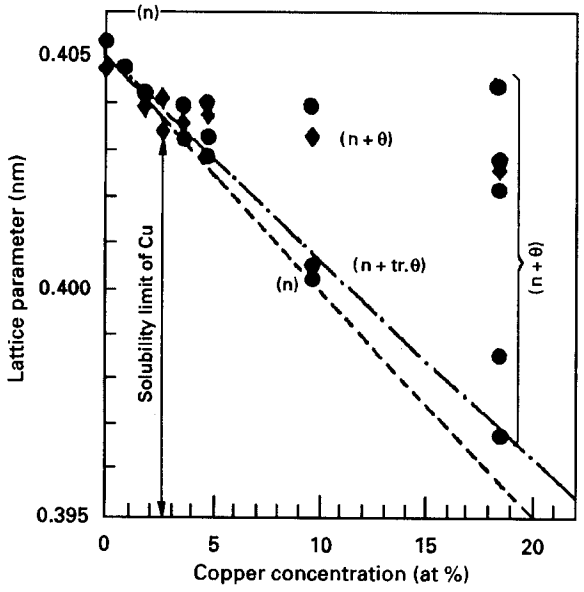

Figure 3 Variation of the lattice parameter of the f.c.c. solid solution of α-Al as a function of composition: (◆) X-ray values, (●) electron microscopy values. The θ phase observed in diffraction is indicated as tr. θ [13].

smaller as compared to the Al–5.94 and 18.29 wt % Cu alloys without any SiC_p.

In order to obtain interplanar distances of the Al–Cu alloys in both the presence and absence of SiC_p high resolution electron microscope (HREM) images were employed. The procedure is based on the measurement of the distance between fringes in the lattice fringe patterns obtained in HREM micrographs. From the values of the interplanar distances, the lattice parameter can be directly obtained. This technique also involves the use of microdensitometer traces taken perpendicular to the lattice fringes. Using

TABLE III Extended solid solution of Cu in α-Al as determined by SEM microanalysis

Experiment	Alloy (wt %)	Cu content in solid solution (wt %)
253	Al–1.34	1.14 ± 0.05
254	Al–5.94	3.62 ± 0.12
255	Al–18.29	7.32 ± 0.21
256	Al–1.47 + SiC_p	1.28 ± 0.08
257	Al–5.95 + SiC_p	3.40 ± 0.16
258	Al–19.43 + SiC_p	6.75 ± 0.12

this approach, the distance between the maxima or minima of these traces can be related with the interplanar distance. In this investigation we have obtained HREM images from four different specimens. Two of these alloy specimens contained SiC particles. Microdensitometer traces have been obtained from the micrographs and subsequently the distances between the lattice fringes were measured. A typical lattice fringe image from the α-Al is shown in Fig. 4. This image has been obtained from a specimen of Al–1.4 wt % Cu + 6 vol % SiC_p and contains fringes that are of the (200) α-Al type. The distance between the fringes was obtained from the quotient between the scale length given by the micrograph mark and the number of maxima or minima in the range of the mark. The value obtained was $d_{(200)} = 0.20235$ nm which gives rise to a lattice parameter value of $a = 0.4047$ nm. Using the same approach, other possible values of the lattice parameter were obtained and for each specimen an average value was finally calculated. With these values and the plot given in Fig. 3, the weight percentage of Cu in solid solution was obtained. These amounts are given in Table IV, where

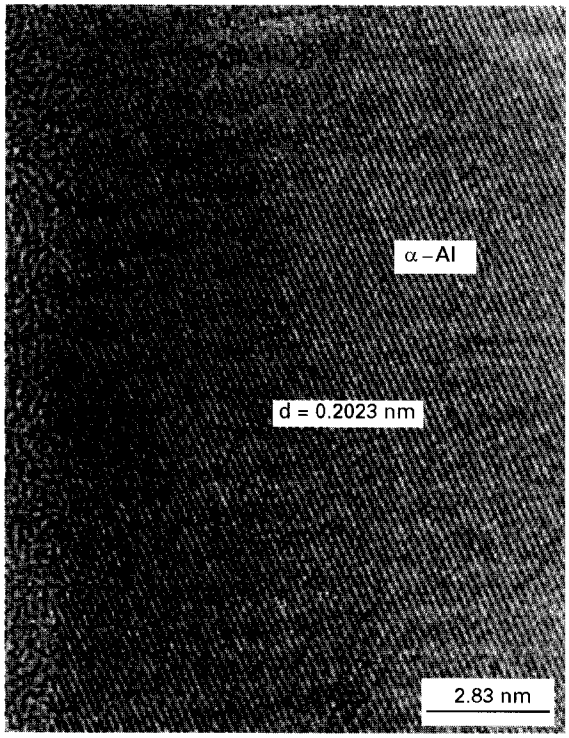

Figure 4 (200) lattice fringes of α-Al. Their corresponding lattice parameter is of the order of $a = 0.4047$ nm.

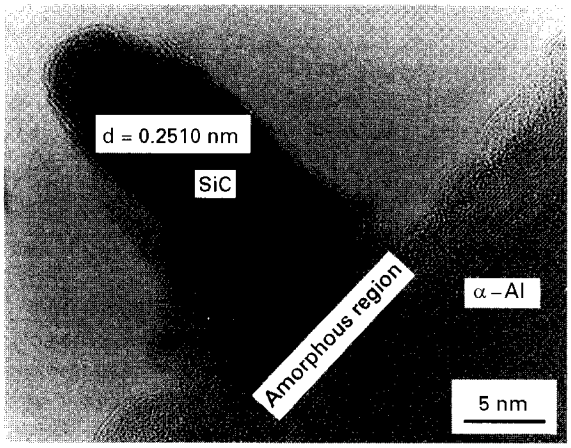

Figure 5 HREM image of the α-Al matrix and a silicon carbide particle. There is an amorphous region surrounding the silicon carbide particle.

the content of Cu in solid solution obtained with the three different methods are summarized. These results indicate that the three different methods give values for the Cu content in the solid solution that closely agree and therefore each of the three techniques can be used for this purpose.

Finally, we would like to draw attention to another image contrast characteristic obtained in the HREM images particularly from those alloys which contain SiC_p. This is illustrated in Figs 5 and 6, where the SiC_p and the Al–Cu matrix can be observed. In most of these images, the carbide particles are found to be surrounded with an amorphous layer a few nanometres wide. This layer, which has not been previously reported, could perhaps be related with the mechanical behaviour of this kind of alloy.

4. Conclusions

(1) It was observed that the mechanisms which define the extent of solid solubility of Cu in Al, in

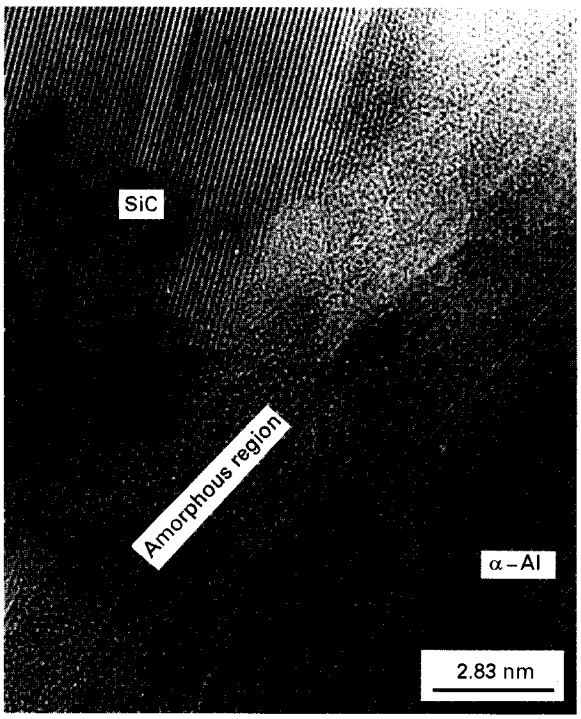

Figure 6 HREM image of the α-Al matrix and a section of a silicon carbide particle. An amorphous region can be observed around the silicon carbide particle.

TABLE IV Solid solution of Cu in α-Al as determined by X-ray diffraction, SEM microanalysis and HREM

Alloy (wt %)	Lattice parameter (nm)	Cu content retained in solid solution obtained by X-ray diffraction (wt %)	Cu content retained in solid solution by microanalysis (wt %)	Cu content retained in solid solution as determined by HREM (wt %)
Al–1.3Cu	0.40484 ± 0.00002	1.07 ± 0.09	1.14 ± 0.05	1.14 ± 0.08
Al–5.9Cu	0.40430 ± 0.00004	3.37 ± 0.19	3.62 ± 0.12	3.56 ± 0.15
Al–18.3Cu	0.40358 ± 0.00004	6.15 ± 0.10	7.32 ± 0.21	—
Al–1.4 Cu + SiC_p	0.40474 ± 0.00002	1.30 ± 0.09	1.28 ± 0.08	1.32 ± 0.11
Al–5.9 Cu + SiC_p	0.40433 ± 0.00004	3.20 ± 0.19	3.40 ± 0.16	3.36 ± 0.20
Al–19.4 Cu + SiC_p	0.40436 ± 0.00004	5.69 ± 0.12	6.75 ± 0.12	—

sprayed-deposited Al–Cu alloys, are controlled by the kinetics during solidification and also modified by the presence of SiC particulates. This was observed from the resulting microstructures and the amount of Cu retained in solid solution in alloys both with and without the addition of SiC_p.

(2) In Al–Cu alloys with low Cu concentrations the SiC_p tend to nucleate in the α-phase, however when the concentration of copper is larger the SiC_p enhance the nucleation of the eutectic phase.

References

1. H. JONES, *Phil. Mag. B* **61** (1990) 487.
2. W. J. BOETTINGER, D. SCHECHTMAN, R. J. SCHAEFER and F. S. BIANCANIELLO, *Metall. Trans. A* **15A** (1984) 55.
3. J. A. JUAREZ-ISLAS, H. JONES and W. KURZ, *Mater. Sci. Engng.* **98** (1988) 201.
4. W. J. BOETTINGER, S. R. CORIELL and R. F. SEKERKA, *ibid.* **65** (1984) 27.
5. F. HEHMANN, F. SOMMER and B. PERDEL, *ibid.* **125** (1990) 249.
6. W. KURZ, B. GIOVANOLA and R. TRIVEDI, *Acta Metall.* **34** (1986) 823.
7. J. A. JUAREZ-ISLAS and H. JONES, in Proceedings of the Solidification Processing Conference Sheffield, UK, September 1987, edited by J. Beach and H. Jones (The Institute of Metals, London, 1988) pp. 492–495.
8. M. J. AZIZ, *J. Appl. Phys.* **53** (1982) 1158.
9. T. R. ANANTHARAMAN and C. SURYANARAYANA, *J. Mater. Sci.* **6** (1991) 1111.
10. F. HEHMANN and H. JONES, in Proceedings of Rapidly Solidified Alloys and their Mechanical and Magnetic Properties Conference, Boston, MA, December 1985, edited by S. Das, B. H. Kear and C. M. Adam (Materials Research Society, Pittsburgh, PA, 1986) **58**, pp. 259–274.
11. E. J. LAVERNIA, *Int. J. Rapid Solidification* **5** (1989) 47.
12. M. GUPTA, F. MOHAMED and E. J. LAVERNIA, *Metall. Trans. A* **23A** (1992) 831.
13. Y. FUJINAGA, S. NAGAKURA and S. OKATANLI, *J. Jpn. Inst. Met.* **32** (1968) 1210.
14. F. H. FROES, Y. W. KIN and S. K. MURTHY, *Mater. Sci. Engng. A* **117** (1989) 831.

Received 25 March 1996
and accepted 28 April 1997